16th World Conference on Earthquake, 16WCEE 2017

Santiago Chile, January 9th to 13th 2017

Paper N° 413

THE JANUARY-FEBRUARY 2014 CEPHALONIA (IONIAN SEA, WESTERN GREECE) EARTHQUAKES: TECTONIC AND SEISMOLOGICAL ASPECTS

S. Mavroulis[(1)], P. Carydis[(2)], V. Alexoudi[(3)], A. Grambas[(4)], E. Lekkas[(5)]

[(1)] *MSc Geologist, Department of Dynamic Tectonic Applied Geology, Faculty of Geology and Geoenvironment, School of Sciences, National and Kapodistrian University of Athens, Greece, smavroulis@geol.uoa.gr*

[(2)] *Professor Emeritus, National Technical University of Athens,Greece, pkary@tee.gr*

[(3)] *MSc Geologist, Department of Dynamic Tectonic Applied Geology, Faculty of Geology and Geoenvironment, School of Sciences, National and Kapodistrian University of Athens, Greece, agram@geol.uoa.gr*

[(4)] *MSc Engineer, Department of Dynamic Tectonic Applied Geology, Faculty of Geology and Geoenvironment, School of Sciences, National and Kapodistrian University of Athens, Greece, valexoudi@geol.uoa.gr*

[(5)] *Professor of Dynamic Tectonic Appleid Geology and Disaster Management, Department of Dynamic Tectonic Applied Geology, Faculty of Geology and Geoenvironment, School of Sciences, National and Kapodistrian University of Athens, Greece, elekkas@geol.uoa.gr*

Abstract

The early 2014 Cephalonia (Ionian Sea, western Greece) earthquake sequence comprised two main shocks with almost the same magnitude (Mw 6.0) occurred successively in short time (January 26, February 3) and space (western Cephalonia, Paliki peninsula). Many earthquake environmental effects (EEE) were induced by both earthquakes in Paliki and classified into primary and secondary. The primary EEE included permanent ground dislocation induced by tectonic uplift and subsidence as well as surface ruptures. The secondary EEE included ground cracks, slope movements, liquefaction and hydrological anomalies. Based on the associated co-seismic surface ruptures, it is concluded that each earthquake was generated onshore by the rupture of a different pre-existing active fault zone in Paliki and produced different co-seismic surface rupture zones. Co-seismic surface rupture structures were strike-slip-related structures including V-shaped conjugate surface ruptures, dextral and sinistral strike-slip surface ruptures, restraining and releasing bends, Riedel structures, small-scale bookshelf faulting and flower structures. From the comparison of all available data including field geological observations, interferometric products and seismological data with the earthquakes effects, it is concluded that there is a strong correlation among the active faults, the detected displacement discontinuities and the spatial distribution of the EEE in the affected area.

Keywords: Active faults; Strike-slip earthquakes; Earthquake environmental effects; ESI 2007 scale; Ionian Islands

1. Introduction

Cephalonia is located only a few km east of the Hellenic Trench in the Ionian Sea, at the northwesternmost part of the Hellenic Arc (Fig. 1a). The Hellenic Trench is an active plate boundary between the subducting eastern Mediterranean lithosphere and the overriding Aegean lithosphere. This subduction zone terminates against the Cephalonia Transform Fault Zone (CTFZ in Fig. 1a) [1, 2]. The CTFZ located west of Lefkas and Cephalonia is composed by the Lefkada segment (LS in Fig. 1b) to the north and the Cephalonia segment (CS in Fig. 1b) to the south. It has a significant role in the geodynamic complexity of the region and the kinematic field in Greece as it (a) connects the subduction boundary to the continental collision between the Hellenic foreland and the Apulian microplate and (b) separates the slowly NNW-ward moving northern Ionian Islands from the rapidly SW-ward moving central Ionian Islands [3, 4, 5].

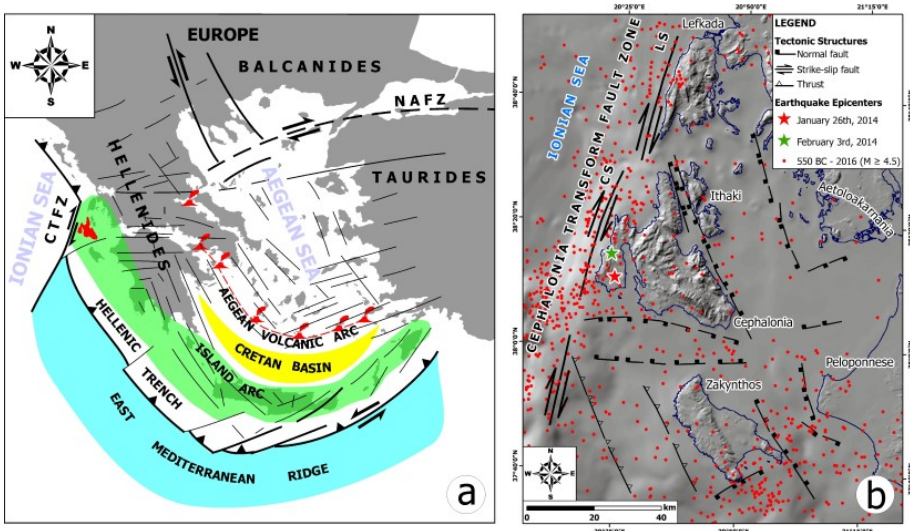

Fig. 1 – (a) Structural sketch of the Hellenic Arc showing the location of the Cephalonia Island at the northwesternmost part of the Hellenic Arc [6, 7]. (b) The central part of the Ionian Islands controlled by the Cephalonia Transform Fault Zone (CTFZ) comprising the Cephalonia segment (CS) and the Lefkada segment (LS). The epicenters of the early 2014 Cephalonia earthquakes (January 26 and February 3) and the epicenters of earthquakes with magnitude ≥ 4.5 for the period extending from 550 BC to April 2, 2016 [8] are also shown.

Due to its location, Ionian Islands are characterized by the highest seismicity in Greece (Fig. 1b). The last episode in the geodynamic evolution of the island was the 2014 January-February earthquake sequence comprising two main shocks with almost the same magnitude occurring successively within short time (January 26 and February 3) and space (western part of Cephalonia). Both shocks were predominantly felt on Cephalonia and throughout the Ionian Islands, the Peloponnese and the Western Continental Greece with fortunately no fatalities or serious injuries reported. Both earthquakes produced extensive earthquake environmental effects which are presented herein.

2. Geological and tectonic setting

Cephalonia comprises alpine formations of Paxoi (Pre-Apulian) and Ionian geotectonic units and Plio-Quaternary sediments that lie on the alpine basement [9, 10, 11, 12, 13, 14, 15, 16, 17 , 18] (Fig. 2). The Paxoi unit occurs in the largest part of the island and consists mainly of neritic and locally pelagic carbonates of Triassic-Middle Miocene age and the flysch-type clay-clastic sequence of Middle Miocene-Early Pliocene age comprising marls, clays, and mudstones in alternations [17, 18] (Fig. 2). The Ionian unit is the allochthonous nappe of the island that occurs along its eastern part (Fig. 2) and comprises an evaporitic sequence of gypsum beds and limestone breccia of Triassic age and thick-bedded limestones, red nodular limestones, and slates of

Jurassic-Cretaceous age [17, 18] (Fig. 2). The recent formations in Cephalonia comprise the Pliocene-Calabrian sequence and the Middle-Late Pleistocene-Holocene formations [17, 18] (Fig. 2).

Four major neotectonic macrostructures constitute the island: (a) the Aenos Mt, (b) the Erissos peninsula, (c) the Paliki peninsula and (d) the Argostoli peninsula (Fig. 2). The Aenos Mt is located in the central and eastern part of Cephalonia and bounded to the SW by the Aenos fault zone, to the NW by the Kontogourata-Agon fault, to the NE by the Agia Efimia fault and to the SE by the Paliokastro fault (AFZ, KAF, AEF, PF respectively in Fig. 2). Aenos Mt has suffered significant uplift (> 1500 meters) and considerable incision since the Early Pliocene [18, 19]. The Erissos peninsula located in the northern part of Cephalonia is bounded to the SW by the AEF and has also suffered significant uplift and erosion. It presents the same evolutional characteristics with the Aenos Mt since Pleistocene and after the deactivation of AEF. The Paliki peninsula located in the western part of the island is bounded to the west by the CTFZ and especially the CS (Fig. 2). This active fault defines the evolution of Paliki through considerable uplift movements (< 1000 meters), which are smaller than the Aenos Mt ones [18, 19]. The Argostoli peninsula located southwest and south of the Aenos Mt is bounded to the east and north by the AFZ (Fig. 2). Back-thrust faults occur exclusively in this macrostructure as the result of possible increased compression during Pleistocene.

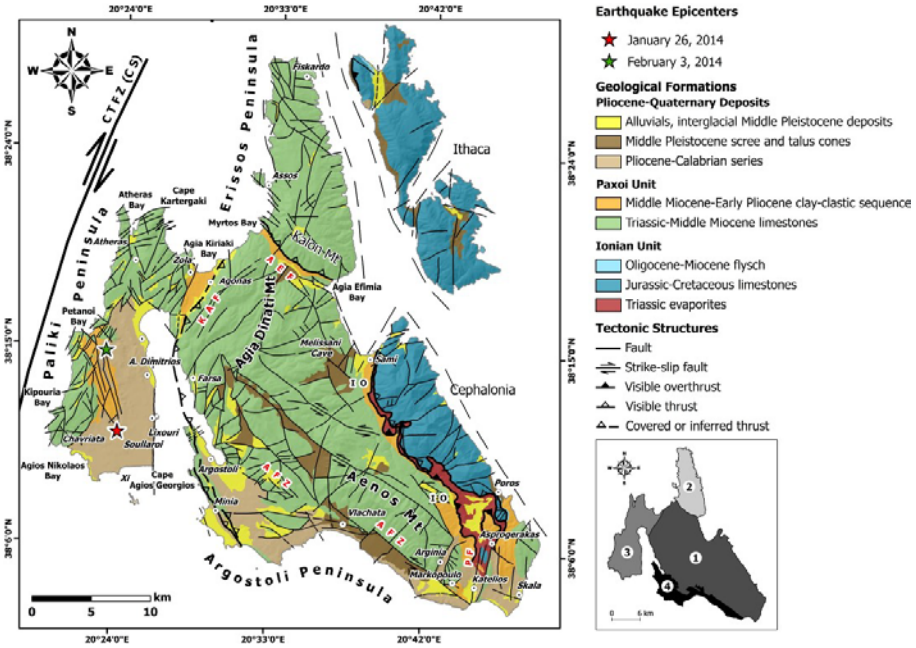

Fig. 2 – Geological map of the Cephalonia Island and its major neotectonic units. (1) Aenos Mt, (2) Erissos peninsula, (3) Paliki peninsula, (4) Argostoli peninsula.

3. Historical seismicity and the 2014 Cephalonia earthquake sequence

The first shock struck on January 26, 2014 at 15:55 (local time) and was assessed as Mw 6.0 (GINOA) or Mw 6.1 (UOA, HARV, INGV, AUTH, GFZ) and the second one on February 3 at 05:08 (local time) was assessed as Mw 5.9 (UOA, GINOA) or Mw 6.0 (HARV, AUTH, GFZ). Despite the fact that the sequence was well recorded by local and regional seismological networks of Greece, the so far published seismological data concerning the epicenter location, the focal depth and the fault plane orientation of both earthquakes [20, 21, 22, 23] present significant variations. This variety indicates not only difficulties in the processing and analyzing data but also stresses the importance of absence of seismological stations from adjacent areas extending west and south of Cephalonia [23]. In this study, the epicenters are relocated and presented onshore [20] (Fig. 3a).

The epicenter of the January 26 earthquake is located onshore in the southeastern part of Paliki peninsula (Fig. 3a). Based on data provided by national and international seismological institutes and observatories (GINOA, UOA, HARV, INGV, AUTH, GFZ), this shock is consistently located at depths of 10-17 km. The

focal mechanism demonstrates a NNE-SSW striking dextral strike-slip seismic fault with a small reverse component that dips southeastwards at a steep angle [20] (Fig. 3a). The aftershock sequence of the first earthquake comprised about 731 events from January 26 to February 3 based on the earthquake catalogues provided by the Permanent Regional Seismological Network operated by the Aristotle University of Thessaloniki, Greece [8] (Fig. 3a). Thirty-one events had magnitude equal to or larger than ML 4.0, with the largest of them measured ML 5.3 and occurred within the first few hours (20:45 local time) after the first shock [8]. The spatial distribution of aftershocks with most hypocentral depths in the range of 1 to 16 km [8] extended for a total length of about 40 km in a NE-SW direction and covered the entire Paliki peninsula (Fig. 3a). This distribution shows consistency with the strike of one of the two nodal planes indicated by the focal mechanisms of the main shock (Fig. 3a).

The February 3 (05:08 local time) earthquake was also generated onshore in the northwestern part of Paliki peninsula (Fig. 3a). It was assessed as Mw 5.9 (UOA, NOA) or Mw 6.0 (HARV, AUTH, GFZ). Its focal depth is about 7 km and its focal mechanism is consistent with NE-SW striking dextral strike-slip [20] (Fig. 3a). Its aftershock sequence comprised 427 seismic events from February 3 to February 13 with most hypocentral depths in the range of 1 to 17 km [8]. Only 14 of them had magnitude equal to or larger than ML 4.0, with the largest one occurring 10 days later [8]. The aftershocks extended for a total length of about 40 km in a NE-SW direction and covered the entire Paliki peninsula once again (Fig. 3a). This direction is again consistent with the strike of one of the two nodal planes indicated by the focal mechanism of the second earthquake (Fig. 3a).

The maximum peak ground acceleration (PGA) of the second shock recorded at Chavriata site (southern Paliki peninsula) was 0.77 g, larger than that recorded during the first shock (0.56 g) [24, 25]. It is significant to note that 0.77 g is the largest PGA value ever recorded in Greece since the early 1970s, when the first accelerographs were installed at large cities of Greece. A slightly smaller PGA was measured as 0.68 g at Lixouri site (eastern coastal Paliki peninsula) during the second event [25].

The historical seismicity and the instrumentally recorded seismological data for the Ionian Islands show that Cephalonia has been repeatedly struck by shocks with magnitudes up to 7.2 and intensity up to X+ (Fig. 3b) and earthquake sequences with more than one strong seismic event [26]. Analogous earthquake sequences have been also generated in 1767 (2 shocks, July 11 and 22), in 1912 (4 shocks, January 24, 25, 26 and February 10), in 1953 (3 shocks, August 9, 11 and 12) and in 1983 (3 shocks, January 17, 19 and March 23) [26] (Fig. 3b). Stress interaction is the most possible explanation for the occurrence mode of strong earthquakes in the Ionian Islands [27]. It is likely that the second main shock of the 2014 Cephalonia sequence was triggered by redistribution and changes of sufficient magnitude in the state of stress following the first main shock [20].

4. Earthquake environmental effects induced by the early 2014 Cephalonia earthquakes

Both earthquakes produced well documented earthquake environmental effects (EEE), which were classified into (a) primary effects directly linked to the earthquake energy and in particular to the surface expression of the seismogenic source and (b) secondary effects induced by the ground shaking (Fig. 4). The first category comprises surface ruptures observed in the field and presented herein as well as permanent ground dislocations induced by tectonic uplift or subsidence and detected by Differential Synthetic Aperture Radar Interferometry (DInSAR) analysis [28] (Fig. 4). The second category comprises ground cracks, slope movements of various types, liquefaction phenomena and hydrological anomalies (Fig. 4).

4.1 Permanent ground dislocation by tectonic uplift and subsidence

Based on surface deformation measurements derived from the application of DInSAR technique for mapping the co- and post-seismic surface deformation caused by the second shock in Cephalonia [28], it is concluded that (a) the central-eastern part of Paliki peninsula suffered uplift ranging from +6 to +12 cm toward the satellite's line of sight (LOS), (b) the northern part of Paliki peninsula and the 600 m wide eastern coastal zone suffered subsidence ranging from -7 to -1 cm, (c) the Argostoli area has subsided [-2.5 cm (LOS)] and (d) the area southeast of Assos village was uplifted by +2.5 cm (LOS) (Fig. 4). The rest of the island displayed minimum surface deformation (Fig. 4).

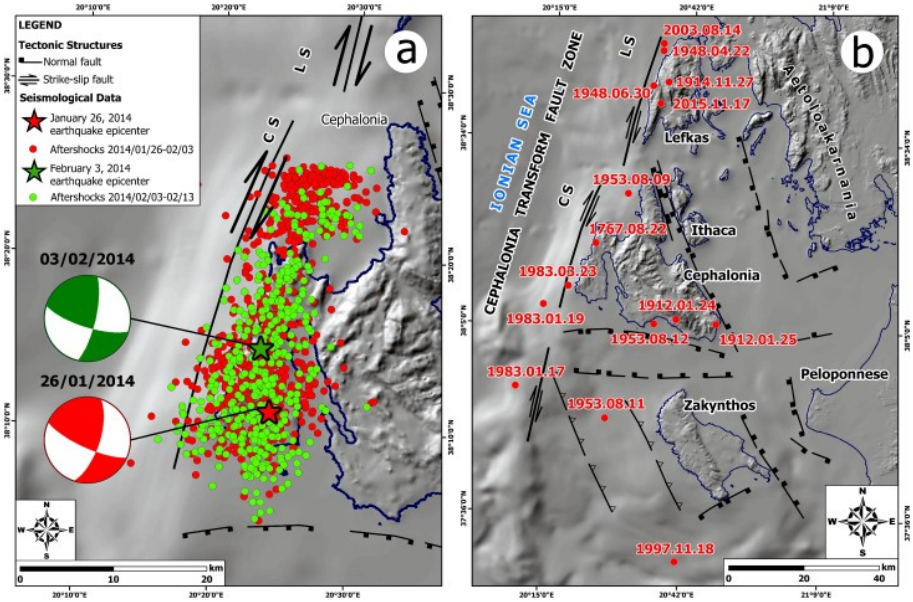

Fig. 3 – (a) Epicenters, focal mechanisms and aftershock distributions of the January 26 and February 3, 2014 Cephalonia earthquakes. (b) Significant historical and instrumentally recorded earthquakes and epicenters that affected the geodynamic evolution of the Ionian Islands.

Based on this interferometric analysis and the resulting surface displacement measurements for the area [28], distinct displacement discontinuities are identified in Paliki peninsula and particularly in its eastern, central and northern part (Fig. 4). Two displacement discontinuities are identified in the eastern coastal part of the Paliki peninsula. The eastern displacement discontinuity is 9 km long and extends from the southeastern end of Paliki to the Agios Dimitrios village (Fig. 4). It juxtaposes the subsided eastern coastal part [-7 cm (LOS) in Agios Dimitrios and -6 cm (LOS) in Lixouri] against the adjacent zone with displacement close to 0 cm (Fig. 4). This displacement discontinuity is most likely to extend northwards below the Livadi bay, reappear in the Livadi swamp and extent with a NE-SW direction until Cape Kartergaki in the northern Paliki, where it juxtaposes a subsided area against an uplifted one (Fig. 4). Another displacement discontinuity is detected to the west of the previous one. It extends with a length of 9 km from the southeastern Paliki to the area south of Livadi village (Fig. 4). It juxtaposes a relatively stable area with displacements close to 0 cm against the central Paliki characterized by maximum uplift (Fig. 4). Some discontinuities are also observed in the central and the northwestern part of Paliki (Fig. 4). Indicatively, an 11-km-long displacement discontinuity extends from the central part of Paliki east of Petanoi bay to Atheras area. It juxtaposes the central Paliki of maximum uplift (+12 cm) against the adjacent western zone with displacement close to 0 cm (Fig. 4).

4.2 Surface ruptures

Surface ruptures were induced by both earthquakes and mainly observed in the northern and central-western part of Paliki. The first earthquake resulted in surface ruptures in the northwestern margin of Thinia valley (Zola area), in the broader area of Livadi swamp and in the area north of Atheras village, while the second earthquake resulted in surface ruptures in the area south of Atheras village and in the area of Petanoi village (Fig. 4).

Surface ruptures in the northwestern margin of Thinia valley were observed in two sites on the road leading from Zola village to Agia Kiriaki bay comprising Paxoi clay-clastic sequence (Fig. 4). V-shaped conjugate surface ruptures striking N10°W and N50°E were observed in the first site with dextral strike-slip offset of 0.5 cm, while N20°E striking surface ruptures were observed in the second site with sinistral strike-slip offset of 7 cm. It is significant to note that they were observed close to a N25°E striking active fault. Their length was up to 20 m, their width ranged from 1 to 5 cm and their depth from 0.5 to 1 m. They caused damage to road asphalt surface, adjacent concrete entrance ramps onto fields and adjacent perimeter stone walls.

Surface ruptures in the broader area of Livadi swamp were observed in three sites and specifically in (a) the area northeast of Livadi swamp comprising Paxoi limestones (Fig. 5a, b), (b) the area close to the eastern end

of Livadi swamp comprising Paxoi limestones and (c) the coastal area of Livadi bay comprising coastal-alluvial deposits (Fig. 4). N20°-30°E striking surface ruptures were observed in the first site with total length up to 300 m, width ranging from 1 cm to 1.5 m, depth from few cm to 1 m, dextral strike-slip offset ranging from 10 to 20 cm and locally vertical offset of 30 cm. N20°E striking surface ruptures were observed in the second site with length of 7 m and were accompanied by N40°W striking minor ruptures. N50°W striking surface ruptures were observed in the third site with length of 10 m resulting in the collapse of the masonry rural prison buildings.

N30°-50°E striking surface ruptures were observed in the area north of Atheras village (Fig. 4) comprising Paxoi limestones with total length of 100 m and width up to 3 m. They were accompanied by positive (palm tree) flower structures (Fig. 5c) and landslides along steep slopes.

N20°-50°E striking surface ruptures were observed in the area south of Atheras (Fig. 4) across a road constructed on Paxoi limestones with length of 10 m, width from 1 to 10 cm, depth from 1 to 20 cm, sinistral offset from 1 to 2.4 cm and vertical offset from 1 to 3 cm. The structure and orientation of these surface ruptures correspond to the upper surficial part of a positive flower structure developed in the area.

Surface ruptures in Petanoi area were induced by the second earthquake and observed in two sites. NW striking surface ruptures were observed close to an active fault juxtaposing Paxoi limestones against the clay-clastic sequence of the same unit. They were 5 m long, 1 cm wide and presented sinistral strike-slip motion. N20°E striking surface ruptures were observed in a rural road constructed on the Paxoi clay-clastic sequence and they presented dextral strike slip. They corresponded to R-bands, synthetic to the sense of shear across the zone, antithetic R′-bands, secondary synthetic P shears, and tensional cracks (T fractures) (Fig. 5d).

The aforementioned surface ruptures are considered primary due to the followings: (a) They were not randomly distributed in the western part of the island but were aligned parallel to and along active faults. (b) They have same orientation with the seismic faults indicated by the earthquakes focal mechanisms. (c) The observed surface ruptures and the accompanied structures showed predominantly dextral strike-slip kinematics with a small normal or reverse component, which is consistent with the type of faulting defined by focal mechanisms. (d) The surface ruptures were traced along displacement discontinuities detected in the eastern, central and northern part of Paliki peninsula based on the interferometric product of Benekos et al. (2015). These distinct displacement discontinuities juxtapose uplifted areas against subsided areas or areas with permanent ground dislocation against stable areas with displacement close to 0 cm and they are the result of local faults activation.

Surface ruptures were not observed in the southern part of the affected area (Fig. 4) despite the extensive structural damage and earthquake environmental effects induced by the first earthquake in Lixouri-Agios Dimitrios area. This fact could be attributed to the unconsolidated or loose character of recent formations of the area, which comprises Pliocene-Calabrian marine and Holocene alluvial and coastal formations.

4.3 Ground cracks

The first earthquake resulted in ground cracks in Myrtos and Agios Nikolaos coastal area (Fig. 4). N30°-50°E and N70°-77°E striking ground cracks were observed on the road passing over the Myrtos beach comprising Paxoi limestones and caused the generation of rock falls and landslides along the cut slopes of the road. A 200-m-long and 60-70-cm-wide ground crack with centimeter-scale normal displacement was also observed along the unstable eastern bank of a river flowing from NE to SW to Agios Nikolaos bay and caused damage on touristic facilities and a concrete river dock along the eastern river bank.

4.4 Slope movements

Numerous slope movements were triggered by both earthquakes in Paliki peninsula and the western and southern parts of Aenos Mt and more specifically (a) landslides, rock falls and rock slides with total volume of 10^3 m^3 in Myrtos coastal area (Fig. 5e), (b) rockfalls, rock toppling failures and landslides with volume smaller than 10^3 m^3 along the margins of Thinia valley, (c) rotational slides, slumps, translational slides, rock falls and rock toppling failures along the route from Argostoli to Lixouri in the western part of Aenos Mt with volume of each movement smaller than 10^3 m^3, (d) rock falls with volume smaller than 10 m^3 in Atheras village, (e) a large-volume ($\simeq 10^3$ m^3) landslide over Petanoi beach (Fig. 5f), (f) landslides and rock falls with volume ranging

from 10 m^3 and 10^3 m^3 along steep slopes in Kipouraioi coastal area and (g) numerous landslides with volume smaller than 10 m^3 along the Xi beach (Fig. 4). Rock falls were also generated at a great distance from the meizoseismal area of both earthquakes in Vlachata area in the southern part of Aenos Mt (Fig. 4). This effect is an isolated effect which occurred in the far field. No slope movements were observed on the rest part of Cephalonia.

Slope movements were mainly generated in areas comprising Triassic-Middle Miocene limestones and Middle Miocene-Early Pliocene clay-clastic sequence of Paxoi unit and Pliocene – Quaternary formations. All sites were high susceptible to slope movements as they all presented suitable and favorable conditions for their generation. These conditions comprise mainly intense tectonic deformation along active faults and multiple fracturing of geological formations resulting in a dense net of discontinuities and sectors of disintegrated geological formations with decreased cohesion and loosening. Moreover, the suitable geometry of discontinuities along high and steep slopes and fault scarps make these areas more susceptible to failure in case of a moderate or large earthquake.

4.5 Liquefaction

Significant liquefaction was not induced by the first earthquake at Lixouri and Argostoli ports (Fig. 4) despite the fact failures including longitudinal cracks parallel to the seashore and displacements of the quay seawalls were mainly occurred in Lixouri port on a large scale and in Argostoli port on a small scale. On the contrary, Lixouri port underwent severe failures during the second shock. Large displacement of the quay seawalls, extensive and various directed longitudinal cracks of the jetties and considerable subsidence, lateral spreading (Fig. 5f) and liquefaction including ejection of sand with gravels of significant size through cracks in several locations. Slight liquefaction phenomena occurred in Argostoli port. Taking into account the fact that Lixouri port was constructed over debris and ruins of houses destroyed during the devastating 1953 Cephalonia earthquakes, it is concluded that liquefaction occurred in the port was non-representative of the actual local soil conditions, the water table and the earthquake loading. Something similar is very likely to have occurred in Argostoli port.

4.6 Hydrological anomalies

Hydrological anomalies were reported in the Lake Cavern of Melissani (Fig. 4), which belongs to the large karstic system of Sami located in the eastern part of Cephalonia. More specifically, water turbidity was reported in the lake. This effect is also considered as an isolated effect occurred in far field.

4.7 ESI 2007 intensities

The Environmental Seismic Intensity (ESI) 2007 scale was applied for seismic intensities assignment to sites where EEE were induced by the 2014 Cephalonia earthquakes [29]. $VIII_{ESI\ 2007}$ intensity was assigned to sites sustained maximum uplift in the central-eastern part of Paliki and $VII_{ESI\ 2007}$ intensity to sites sustained maximum subsidence, surface ruptures and large-volume slope movements in the eastern coastal zone of Paliki, the northern part of Paliki and the northern part of Argostoli peninsula, respectively. $VI_{ESI\ 2007}$ intensity was assigned to sites with ground cracks and slope movements generated mainly in the northern part of Paliki and the western part of Aenos Mt, respectively. $V_{ESI\ 2007}$ intensity was assigned to small-volume slope movements generated in the southern part of Paliki.

5. Fault zones ruptured during the 2014 Cephalonia earthquakes

Based on the abovementioned direct field observations immediately after each earthquake, it is revealed that each earthquake was generated onshore by the rupture of a different pre-existing active fault zone in Paliki peninsula (Fig. 6a). The first event was generated by the rupture of a fault zone located in the eastern and northwestern part of Paliki peninsula. The southern part of this fault zone has length of about 18 km extending from the Cape Agios Georgios in the southeastern end of Paliki peninsula to Agia Kyriaki bay in the northeastern part of the same macrostructure (Fig. 6a). It could be segmented into three parts considering their morphological characteristics and the geometry of tectonic structures as well as the geometry, the slip distribution and the kinematics of the observed surface ruptures.

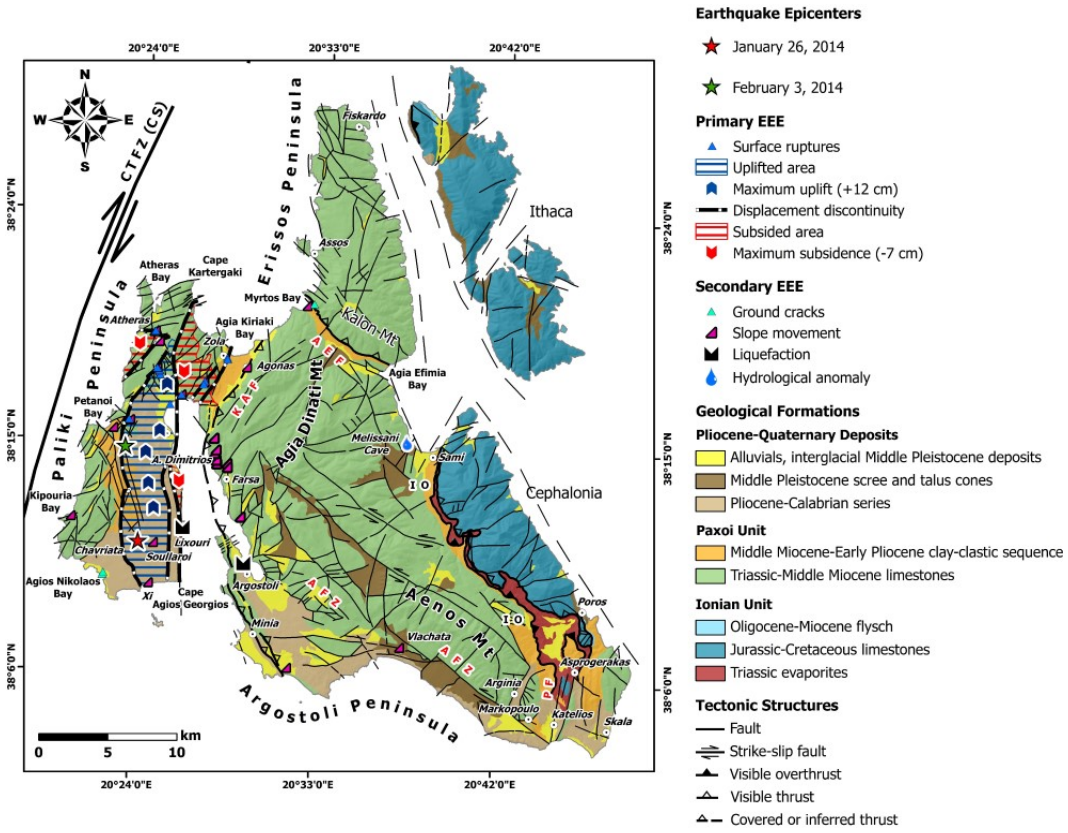

Fig. 4 – Distribution of the earthquake environmental effects induced by the 2014 Cephalonia earthquakes.

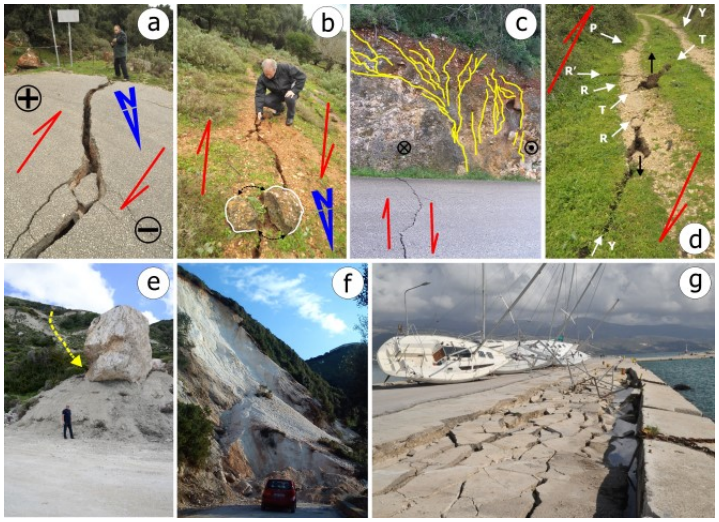

Fig. 5 – (a, b) Surface ruptures in the area northeast of the Livadi swamp resulting in destruction of the road asphalt surface. Restraining and releasing bends due to minor changes in fault trend were observed along the surface rupture zone. (c) Positive flower structure due to the small reverse component along surface ruptures induced by the January 26, 2014 and observed in the area north of Atheras village. (d) Co-seismic surface rupture structures observed in Petanoi area. (e, f) Rockfalls in Myrtos beach and landslides in Petanoi beach induced by the first and the second event respectively. (g) Liquefaction-induced lateral spreading in Lixouri port.

The first segment is 10 km long and extends from the southeastern tip of Paliki (Cape Agios Georgios) to Agios Dimitrios area (Fig. 6a). It is composed of a straight N-S striking active fault with considerable strike-slip component forming the southeastern coastal part of Paliki and juxtaposing the Pliocene-Calabrian marine sequence against the recent deposits of the Livadi bay and the alluvial deposits of Agios Dimitrios coastal plain

(Fig. 6a). The second segment extends from north of Agios Dimitrios area to Livadi swamp (Fig. 6a). The abovementioned active fault zone is most likely to extend along the almost N-S striking morphological escarpment that follows approximately the contact between the Pliocene-Calabrian marine sequence and the recent deposits of the Livadi village coastal area located westwards and deeper below the Livadi bay located northwards (Fig. 6a). Villages nearby this morphological escarpment underwent serious damage by both earthquakes. The Lixouri – Agios Dimitrios area located nearby the first fault segment underwent serious damage by the first earthquake, while villages located close the second segment suffered considerable damage by both earthquakes. In spite of these effects on the natural and the built environment of the aforementioned areas, distinct surface ruptures were not detected in the field mainly due to the unconsolidated and loose geological formations comprising Plio-Quaternary marine formations and alluvial as well as coastal deposits.

The third segment extends from the Livadi swamp to the Zola area in the northwestern margin of the Thinia valley. The aforementioned active fault zone comprises NE-SW striking strike-slip faults disrupting Triassic-Middle Miocene limestones of the Paxoi unit or juxtaposing these limestones against the Middle Miocene-Early Pliocene clay-clastic sequence of the same unit (Fig. 6a).

The co-seismic strike-slip-related structures associated with the first earthquake were observed along the third segment and especially in Zola and Livadi broader areas (Fig. 6a). They included V-shaped conjugate surface ruptures, surface ruptures indicating right-lateral strike-slip faulting, restraining and releasing bends, Riedel structures, and small-scale bookshelf faults. The presence of ground openings (sinkholes), small grabens and dip-slip displacements in the same area reveals the existence of an extensional component across this surface rupture zone. Co-seismic displacements were determined by offset surface markers, namely roads and paths crossing the co-seismic surface rupture zone. In Zola, the co-seismic dextral offset was of 0.5 cm, while the sinistral offset ranged from 1.4 to 7 cm. In Livadi, the co-seismic dextral offset ranged from 10 to 20 cm, while the maximum vertical offset determined by dip-slip displacements was of about 30 cm.

The northwestern part of the fault zone ruptured during the first earthquake has a length of 4 km extending from south of Atheras village to Atheras bay area in an N-S direction (Fig. 6a) and consists of faults disrupting the Triassic-Middle Miocene limestones of Paxoi unit. The co-seismic surface rupture structures associated with the first earthquake indluded surface structures indicating strike-slip faulting and flower structures revealing a reverse component in the movement. The determined co-seismic dextral offset was 2 cm along structures observed north of the Atheras village.

The second event was generated by the rupture of a NNE-SSW striking fault zone in the western part of Paliki and could be segmented into two parts considering the abovementioned segmentation criteria (Fig. 6a). The first segment has length of about 12 km, extends from southwest of the Chavriata village to the Agia Thekli area (Fig. 6a) and comprises NNE-SSW and NE-SW striking active faults separating fault blocks with different dominant geological formations . The western fault block consists mainly of Triassic-Middle Miocene limestones of Paxoi unit, while the eastern fault block is composed mainly of the Pliocene-Calabrian sequence (Fig. 6a). It is important to note that the maximum peak ground acceleration during the 2014 Cephalonia earthquake sequence was recorded close to the Chavriata village [24, 25]. Co-seismic surface rupture structures and in particular surface ruptures indicating strike-slip faulting were also observed in this segment in Petanoi area (Fig. 6a).

The second segment extends from the area north of Agia Thekli to the Cape Kartergaki (Fig. 6a) in the northern part of Paliki and comprises NE-SW and E-W striking active faults that disrupt Triassic-Middle Miocene limestones of the Paxoi unit and reveal significant dextral strike-slip motion [17, 18]. Co-seismic surface rupture structures were also observed in this segment in the area south of the Atheras village and comprised surface ruptures indicating strike-slip faulting, Riedel structures, and flower structures revealing a compressional component across this surface rupture zone. The sinistral offset of these structures ranged from 1 to 2.4 cm, while the vertical offset ranged from 1 to 3 cm.

6. Conclusions

From the comparison of the field geological observations in Cephalonia Island immediately after each earthquake with the aforementioned DInSAR analysis results and the detected displacement discontinuities, it is concluded that there is a strong correlation among the ruptured active fault zones, the surface rupture zones, and the detected displacement discontinuities in Paliki peninsula (Fig. 6a,b). The fault zone ruptured in the first earthquake coincides with the surface rupture zone in the northeastern part of Paliki peninsula and the displacement discontinuities detected in the eastern part of the island that juxtapose areas with different permanent ground dislocations (uplifted against subsided) or areas with permanent ground dislocation against stable areas (Fig. 6a,b). The fault zone ruptured in the second earthquake coincides with the surface rupture zone in Petanoi and southern Atheras areas and the displacement discontinuities detected in the central and northwestern part of the island that juxtapose uplifted against stable areas (Fig. 6a,b).

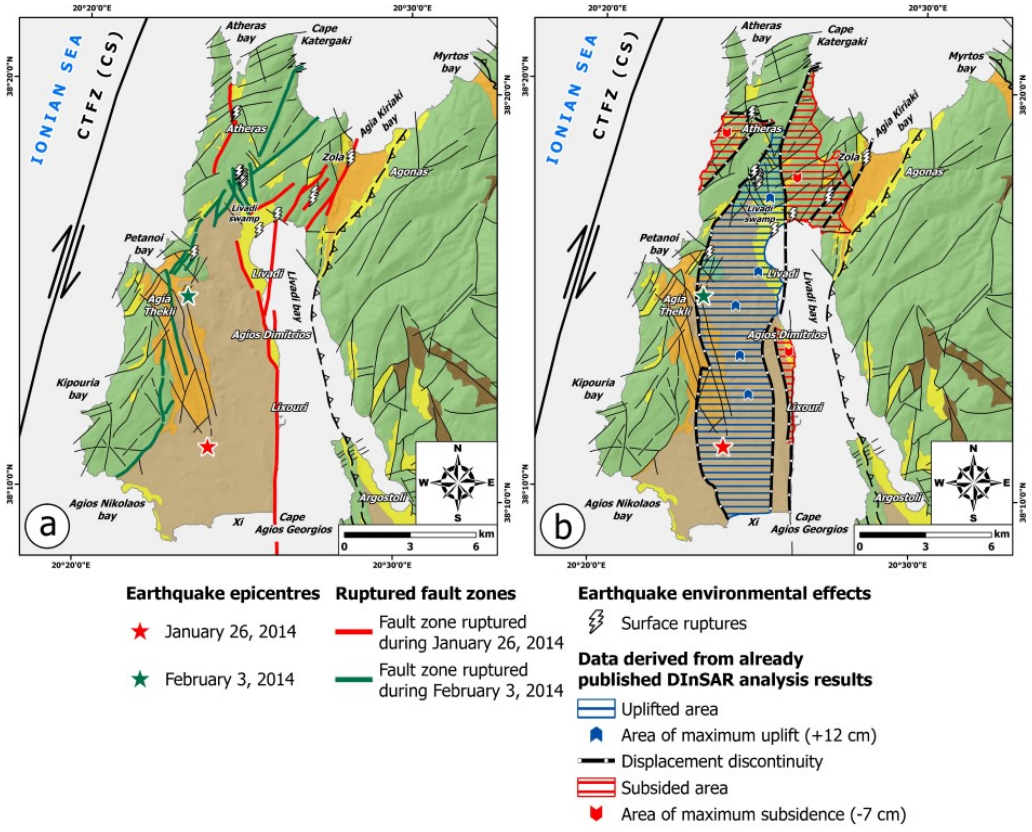

Fig. 6 – Strong correlation among the (a) geological field data (ruptured active fault zones and surface rupture zones) and (b) displacement discontinuities derived from surface deformation measurements [28].

Taking into account the type and the dimensional characteristics of the EEE induced by the 2014 Cephalonia earthquake sequence as well as the seismic intensities assigned to the these effects [29], it is concluded that the worst affected areas of Cephalonia were primarily the Paliki peninsula and secondarily the western part of Aenos Mt and the northern part of the Argostoli peninsula (Fig. 7) with the highest assigned seismic intensities (intensities equal to $VIII_{ESI\ 2007}$ and $VII_{ESI\ 2007}$) [29]. The less affected parts of the island were the Erissos peninsula in its entirety, the central and eastern part of Aenos Mt and the central and eastern part of the Argostoli peninsula (intensities equal to or lower than $V_{ESI\ 2007}$) (Fig. 7). In total, almost 20000 residents in Paliki and Argostoli areas were exposed to seismic intensities ranging from VI to VIII, while almost 4500 residents were exposed to the maximum seismic intensity (VIII).

From the comparison of the above mentioned seismic intensity distribution with historical earthquake intensity data for Cephalonia [26, 30, 31], it becomes clear that this is not the first time such a distribution is observed on the island. The western part of the island is the area usually and mostly affected by earthquake

effects in its natural and built environment (Fig. 7). More specifically, the highest seismic intensities of historical earthquakes have undoubtedly been observed in the western part of Cephalonia in general and in Paliki peninsula in particular (IX-X_{+MMI} during the 1658, 1767, 1867 and 1953 earthquakes) (Fig. 7). On the contrary, Erissos peninsula is the only neotectonic macrostructure of the island that suffered the lowest seismic intensities during these shocks (IV-VI_{MMI} during the 1658, 1767, 1862, 1867, 1915 and 1953 earthquakes) (Fig. 7). This anomalous attenuation of seismic waves is generally correlated with the geodynamic complexity of the region and strongly related with the complexity of fault systems and the existence of salt layers that lie into the adjacent slipping areas of the faults [30, 31].

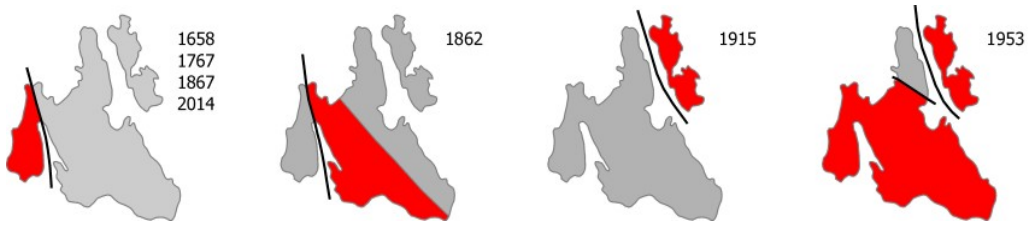

Fig. 7 – Areas with high contrasts in seismic intensities during major earthquakes in Cephalonia. The highest intensities have undoubtedly been observed in the Paliki peninsula (IX-$X+_{MMI}$ during the 1658, 1767, 1867, 1953 and 2014 earthquakes). On the contrary, the Erissos peninsula is the only macrostructure that suffered low intensities (IV-VI_{MMI} during the 1658, 1767, 1862, 1867, 1915, 1953 and 2014 earthquakes) [31, this study].

6. References

[1] Scordilis EM, Karakaisis GF, Karacostas BG, Panagiotopoulos DG, Comninakis PE, Papazachos BC (1985): Evidence for transform faulting in the Ionian Sea: the Cephalonia island earthquake sequence of 1983. *Pure and Applied Geophysics*, 123, 388-397.

[2] Louvari E, Kiratzi A, Papazachos BC (1999): The Cephalonia transform fault and its extension to western Lefkada Island (Greece). *Tectonophysics*, **308**, 223-236.

[3] Anzidei M, Baldi P, Casula G, Crespi M, Riguzzi F (1996): Repeated GPS surveys across the Ionian Sea: evidence of crustal deformations. *Geophysical Journal International*, **127**, 257-267.

[4] Hollenstein CH, Geiger A, Kahle H-G, Veis G (2006): CGPS time-series and trajectories of crustal motion along the West Hellenic Arc. Geophysical Journal International, 164(1), 182-191.

[5] Hollenstein CH, Müller MD, Geiger A, Kahle H-G (2008): Crustal motion and deformation in Greece from a decade of GPS measurements 1993–2003. *Tectonophysics*, **449**, 17-40.

[6] Mariolakos I, Papanikolaou D (1981): The neogene basins of the Aegean Arc from the paleogeographic and the geodynamic point of view. In: Proceedings of the International Symposium Hellenic Arc and Trench (HEAT), I, pp. 383-399

[7] Mariolakos I, Papanikolaou D (1987): Deformation pattern and relation between deformation and seismicity in the Hellenic arc. *Bulletin of the Greek Geological Society*, **19**, 59-76.

[8] Aristotle University of Thessaloniki (AUTH) (2016): Permanent Regional Seismological 960 Network operated by the Aristotle University of Thessaloniki, doi:10.7914/SN/HT

[9] Renz C (1955): Die vorneogene stratigraphia der normalsedimentaren formationen Griechenlands. In: IGSR (ed), Athens, p. 637.

[10] Aubouin J (1959): Contribution a l' étude géologique de la Grèce septentrionale, les confins de l'Epire et de la Thessalie. *Annales Géologiques des Pays Hélléniques*, **10**, 1-525.

[11] Aubouin J, Dercourt J (1962): Zone preapulienne, zone ionienne et zone du Gavrovo en Peloponncse occidentale. *Bulletin de la Société géologique de France*, 4, 785-794.

[12] Georgiadou-Dikaioulia E (1967): *The Neogene of Kephallinia*. PhD Thesis, University of Athens.

[13] BP Co (1971): *The geological results of petroleum exploration in Western Greece*. Institute of Geology and Subsurface Research, Athens, 10, p. 73.

[14] BP Co, University of Munich, Migiros G (1985): *Geological map of Greece, "Cephalonia Island (Northern and southern part)'', 1:50000 scale*. IGME, Athens.

[15] Stavropoulos A (1988): *Geological map of Greece, ''Ithaki-Atokos'', 1:50000 scale*. IGME, Athens.

[16] Underhill JR (1989): Late Cenozoic deformation of the Hellenide foreland, western Greece. *Bulletin of the Geological Society of America*, 101, 613-634.

[17] Lekkas E (1996): *Neotectonic Map of Greece. Cephalonia—Ithaki sheet. Scale 1:100.000*. University of Athens.

[18] Lekkas E, Danamos G, Mavrikas G (2001): Geological structure and evolution of Cefallonia and Ithaki Islands. *Bulletin of the Geological Society of Greece*, **34** (1), 11-17.

[19] Sorel D (1976): *Etude Néotectonique des îles Ioniennes de Céphalonie et de Zante et de l' Elide Occidentale (Grèce)*.Thèse 3e cycle, Orsay, Université Paris Sud, p. 200.

[20] Karakostas V, Papadimitriou E, Mesimeri M, Gkarlaouni Ch, Paradisopoulou P (2014). The 2014 Kefalonia Doublet (Mw 6.1 and Mw 6.0), Central Ionian Islands, Greece: Seismotectonic Implications along the Kefalonia Transform Fault Zone. *Acta Geophysica*, DOI: 10.2478/s11600-014-0227-4

[21] Papadopoulos GA, Karastathis VK, Koukouvelas I, Sachpazi M, Baskoutas I, Chouliaras G, Agalos A, Daskalaki E, Minadakis G, Moshou A, Mouzakiotis A, Orfanogiannaki K, Papageorgiou A, Spanos D, Triantafyllou I (2014): The Cephalonia, Ionian Sea (Greece), sequence of strong earthquakes of January–February 2014: a first report. *Research in Geophysics*, **4**:5441. http://dx.doi.org/10.4081/rg.2014.5441

[22] Boncori JPM, Papoutsis I, Pezzo G, Tolomei C, Atzori S, Ganas A, Karastathis V, Salvi S, Kontoes C, Antonioli A. (2015): The February 2014 Cephalonia earthquake (Greece): 3D deformation field and source modeling from multiple SAR techniques. *Seismological Research Letters*, **86** (1), 124-137. http://dx.doi.org/10.1785/0220140126

[23] Sokos E, Kiratzi A, Gallovič F, Zahradník J, Serpetsidaki A, Plicka V, Janský J, Kostelecký J, Tselentis G-A (2015): Rupture process of the 2014 Cephalonia, Greece, earthquake doublet (Mw6) as inferred from regional and local seismic data. *Tectonophysics*, **656**, 131–141, doi:10.1016/j.tecto.2015.06.013

[24] Karakostas Ch, Lekidis V, Makra K, Margaris B, Morfidis K, Papaioannou Ch, Rovithis M, Salonikios T, Savvaidis A, Theodoulidis N (2014a): The earthquake of 26/1/2014 (M6.1) in Cephalonia (Greece): strong ground motion, soil behaviour and response of structures (preliminary report). *Report*, Earthquake Planning and Protection Organization – Institute of Engineering Seismology and Earthquake Engineering. Thessaloniki, Greece. http://www.slideshare.net/itsak-eppo/20140126-kefaloniaeq-report-en Accessed April 2014

[25] Karakostas Ch, Lekidis V, Makra K, Margaris B, Morfidis K, Papaioannou Ch, Rovithis M, Salonikios T, Savvaidis A, Theodoulidis N (2014b): Strong ground motion of the February 3, 2014 (M6.0) Cephalonia earthquake: effect on soil and built environment in combination with the January 26, 2014 (M6.1) event. *Report*, Earthquake Planning and Protection Organization - Institute of Engineering Seismology and Earthquake Engineering. Thessaloniki, Greece. http://www.slideshare.net/itsak-eppo/20140203-kefaloniaeq-report-en Accessed April 2014

[26] Papazachos B, Papazachou C (2003): *The Earthquakes of Greece*. Ziti Publ., Thessaloniki.

[27] Papadimitriou EE (2002): Mode of strong earthquake recurrence in the central Ionian Islands (Greece): possible triggering due to Coulomb stress changes generated by the occurrence of previous strong shocks. *Bulletin of the Seismological Society of America*, **92** (8), 3293-3308.

[28] Benekos G, Derdelakos K, Bountzouklis C, Kourkouli P, Parcharidis I (2015): Surface displacements of the 2014 Cephalonia (Greece) earthquake using high resolution SAR interferometry. *Earth Science Informatics*, 8, 309-315, DOI 10.1007/s12145-015-0205-7.

[29] Lekkas EL, Mavroulis SD (2015): Earthquake environmental effects and ESI 2007 seismic intensities of the early 2014 Cephalonia (Ionian Sea, western Greece) earthquakes (January 26 and February 3, Mw 6.0). *Natural Hazards*, **78**, 1517-1544.

[30] Stiros S (1994): Anomalous attenuation of seismic waves in the Ionian islands, Greece. *Transactions - American Geophysical Union*, **75**, 117-118.

[31] Stiros SC, Pirazzoli PA, Laborel J, Laborel-Deguen F (1994): The 1953 earthquake in Cephalonia (Western Hellenic Arc): coastal uplift and halotectonic faulting. *Geophysical Journal International*, 117, 834-849.